A kinetic study of thiol addition to *N*-phenylchloroacetamide

Sarah K. I. Watt[a], Janique G. Charlebois[a], Christopher N. Rowley[b], Jeffrey W. Keillor[a]*

[a]Department of Chemistry and Biomolecular Sciences, University of Ottawa, Ottawa, Canada

[b] Department of Chemistry, Carleton University, Ottawa, Canada

***Corresponding author:** jkeillor@uottawa.ca

Table of Contents **Page**

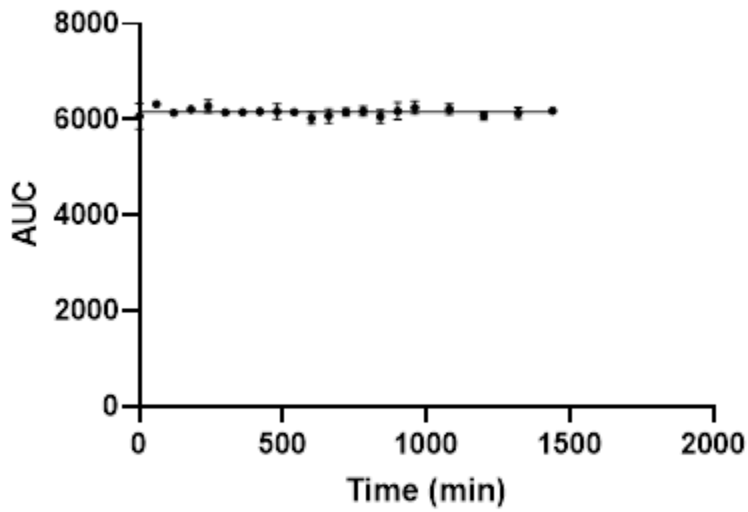

Figure S1. Stability of 1 mM NPC in aqueous buffer, pH=7.4, assessed over 24 hours. Data were fit to a linear regression to obtain a slope of -0.029 ± 0.042 that is not statistically significant from zero, *P* value = 0.4998, and y-intercept of 6179 ± 31.

Table S1. pH of buffer, mobile phase gradient, length of run and retention times of NPC and thiol-adduct for each experiment of NPC with RSH (**1a-d**).

Thiol	[NPC] mM	[Thiol] mM	pH of Aqueous Buffer	Mobile Phase Gradient (% CH_3CN in H_2O)	Total Length of Run (min)	Retention Time NPC (min)	Retention Time Adduct (min)
1a	2	20	6.80	20-80	15	8.6	4.5
1b	1	10	7.40	18-30	20	11.9	3.3
1c	2	20	8.00	20-80	15	8.6	5.8
1d	1	10	9.01	18-30	20	11.9	10.8

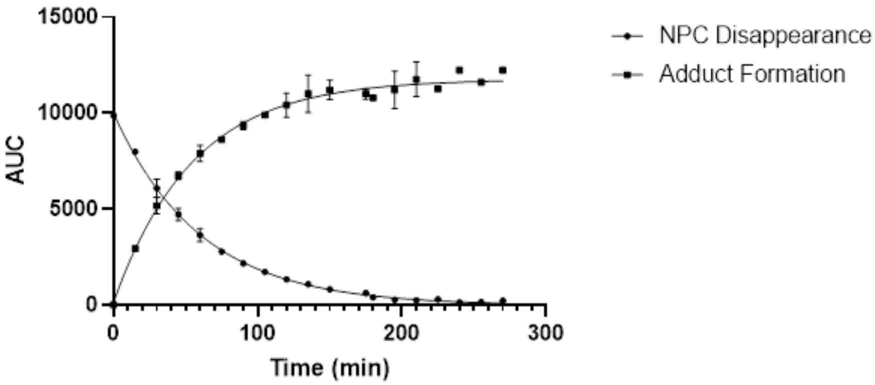

Figure S2. Plot of disappearance of NPC (2 mM) and formation of adduct for the addition of DEC (20 mM) vs time (min) in 67 mM MOPS buffer (1% v/v DMSO), pH 6.8, μ = 0.100, T = 22°C. The area under the curve (AUC) was integrated from the chromatograph at 214 nm for the peaks corresponding to NPC and the adduct. The AUC data for disappearance of NPC were fitted to a mono-exponential decay with the constraint that the plateau = 0 and the data for formation of adduct were fitted to a mono-exponential association to afford the k_{obs} values summarized in **Table S2**.

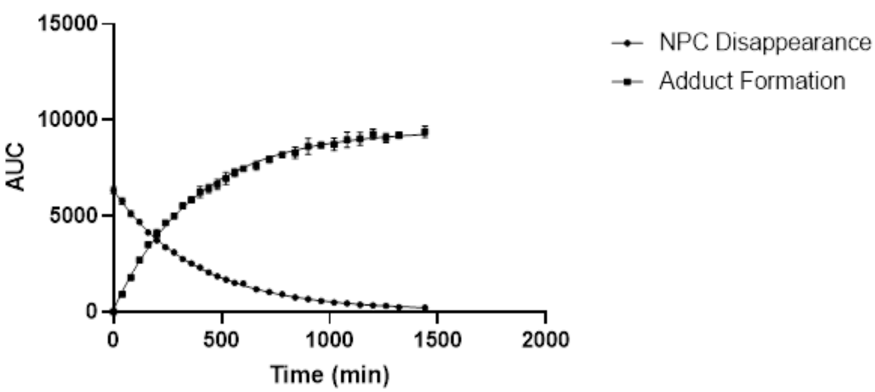

Figure S3. Plot of disappearance of NPC (1 mM) and formation of adduct for the addition of GSH (10 mM) vs time (min) in 67 mM potassium phosphate buffer (0.5% v/v DMSO), pH 7.4, μ = 0.100, T = 22°C. The area under the curve (AUC) was integrated from the chromatograph at 214 nm for the peaks corresponding to NPC and the adduct. The AUC data for disappearance of NPC were fitted to a mono-exponential decay with the constraint that the plateau = 0 and the data for formation of adduct were fitted to a mono-exponential association with the constraint that $Y_0 = 0$ to afford the k_{obs} values summarized in **Table S2**.

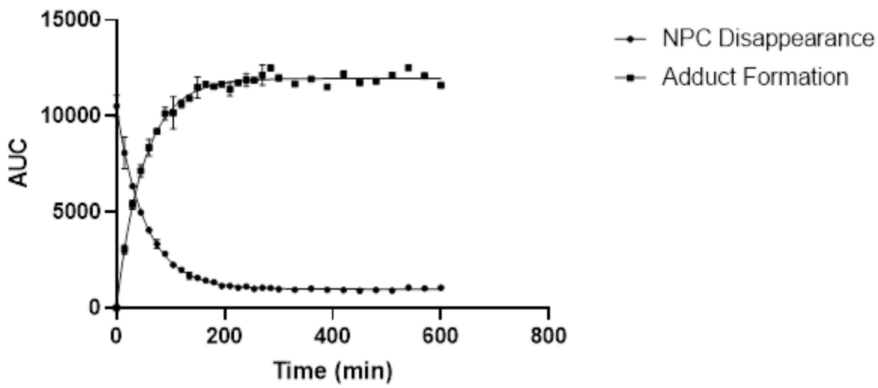

Figure S4. Plot of disappearance of NPC (2 mM) and formation of adduct for the addition of BME (20 mM) vs time (min) in 67 mM Tris buffer (1% v/v DMSO), pH=8.0, μ=0.100, T=22°C. The area under the curve (AUC) was integrated from the chromatograph at 214 nm for the peaks corresponding to NPC and the adduct. The AUC data for disappearance of NPC were fitted to a mono-exponential decay with the constraint that the plateau = 0 and the data for formation of adduct were fitted to a mono-exponential association with the constraint that $Y_0 = 0$ to afford the k_{obs} values summarized in **Table S2**.

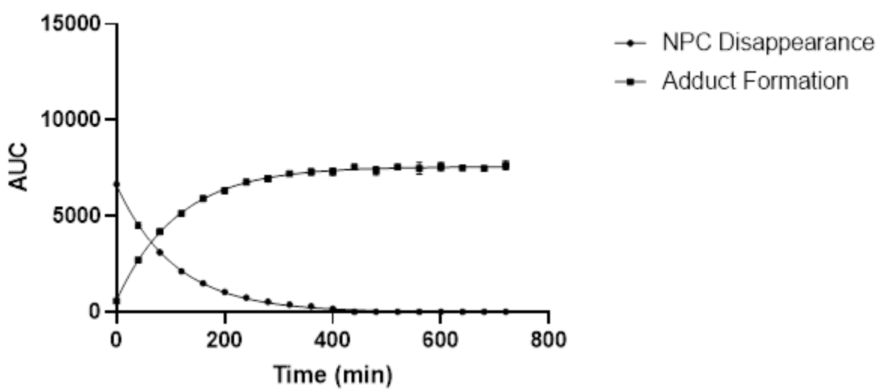

Figure S5. Plot of disappearance of NPC (1 mM) and formation of adduct for the addition of MPA (10 mM) vs time (min) in 67 mM CHES buffer (1% v/v DMSO), pH=9, μ=0.100, T=22°C. The area under the curve (AUC) was integrated from the chromatograph at 214 nm for the peaks corresponding to NPC and the adduct. The AUC data for disappearance of NPC were fitted to a mono-exponential decay with the constraint that the plateau = 0 and the data for formation of adduct were fitted to a mono-exponential association with the constraint that $Y_0 = 0$ to afford the k_{obs} values summarized in **Table S2**.

Table S2. Observed rate constants (k_{obs}), calculated second order rate constants (k_2^{calc}), and corrected second order rate constants (k_2^{corr}) for the addition of RSH (**1a-d**) to NPC. Measurements were made in duplicate for both the disappearance of chloroacetamide and appearance of adduct, providing quadruplicate measurements. Errors shown for k_{obs} and k_2^{calc} represent the standard error of the fitting. The errors shown for k_2^{calc} represent the propagated uncertainty including the uncertainty in f RS^- (see Table 2).

Thiol	k_{obs} (10^{-3} s^{-1})	k_2^{calc} ($M^{-1}s^{-1}$)	k_2^{corr} ($M^{-1}s^{-1}$)	$\log(k_2^{corr})$
1a	0.2722 ± 0.0046	0.01361 ± 0.00023	0.150 ± 0.039	-0.825 ± 0.131
1a	0.2877 ± 0.0045	0.01491 ± 0.00023	0.158 ± 0.041	-0.801 ± 0.131
1a	0.3532 ± 0.0254	0.01766 ± 0.00127	0.194 ± 0.052	-0.712 ± 0.137
1a	0.2798 ± 0.0135	0.01399 ± 0.00068	0.154 ± 0.041	-0.813 ± 0.134
1b	0.04237 ± 0.00031	0.004237 ± 0.000031	0.0813 ± 0.0101	-1.090 ± 0.058
1b	0.04178 ± 0.00037	0.004178 ± 0.000037	0.0802 ± 0.0100	-1.096 ± 0.058
1b	0.04450 ± 0.00085	0.004450 ± 0.000085	0.0854 ± 0.0107	-1.068 ± 0.058
1b	0.04468 ± 0.00086	0.004468 ± 0.000086	0.0858 ± 0.0108	-1.067 ± 0.058
1c	0.3308 ± 0.0061	0.01654 ± 0.00031	0.645 ± 0.083	-0.190 ± 0.060
1c	0.2955 ± 0.0175	0.01478 ± 0.00087	0.577 ± 0.081	-0.239 ± 0.066
1c	0.3392 ± 0.0056	0.01696 ± 0.00028	0.662 ± 0.085	-0.179 ± 0.060
1c	0.3137 ± 0.0096	0.01568 ± 0.00048	0.612 ± 0.080	-0.213 ± 0.061
1d	0.1548 ± 0.0018	0.01548 ± 0.00018	0.297 ± 0.037	-0.527 ± 0.058
1d	0.1574 ± 0.0020	0.01574 ± 0.00020	0.302 ± 0.038	-0.520 ± 0.058
1d	0.1599 ± 0.0061	0.01599 ± 0.00061	0.307 ± 0.040	-0.513 ± 0.060
1d	0.1663 ± 0.0064	0.01663 ± 0.00064	0.319 ± 0.041	-0.496 ± 0.060

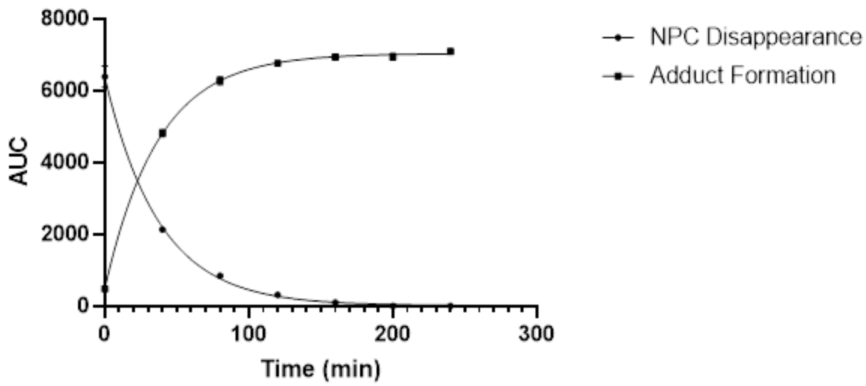

Figure S6. Plot of disappearance of NPC (1 mM) and formation of adduct for the addition of 1d (10 mM) vs time (min) in 67 mM CHES buffer (0.5% v/v DMSO) at pH 9.0, μ = 0.100, T = 37°C. The area under the curve (AUC) was integrated from the chromatograph at 214 nm for the peaks corresponding to NPC and the adduct. The AUC data for disappearance of NPC were fitted to a mono-exponential decay with the constraint that the plateau = 0 and the data for formation of adduct were fitted to a mono-exponential association with the constraint that $Y_0 = 0$ to afford the k_{obs} values summarized in **Table S3**.

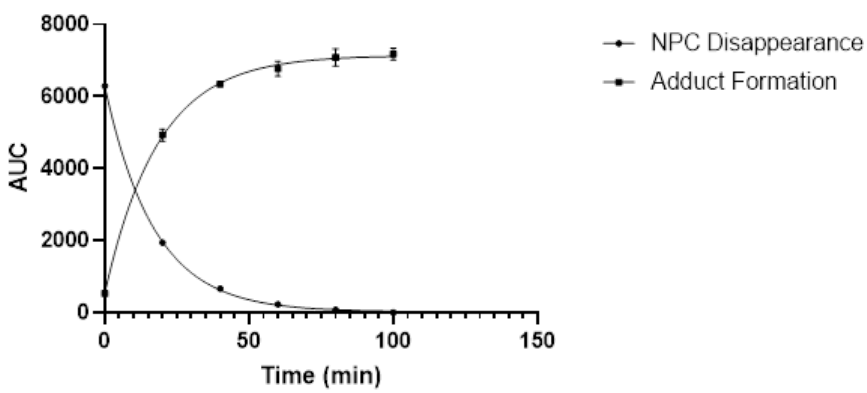

Figure S7. Plot of disappearance of NPC (1 mM) and formation of adduct for the addition of 1d (10 mM) vs time (min) in 67 mM CHES buffer (0.5% v/v DMSO) at pH 9.0, μ = 0.100, T = 53°C. The area under the curve (AUC) was integrated from the chromatograph at 214 nm for the peaks corresponding to NPC and the adduct. The AUC data for disappearance of NPC were fitted to a mono-exponential decay with the constraint that the plateau = 0 and the data for formation of adduct were fitted to a mono-exponential association with the constraint that $Y_0 = 0$ to afford the k_{obs} values summarized in **Table S3**.

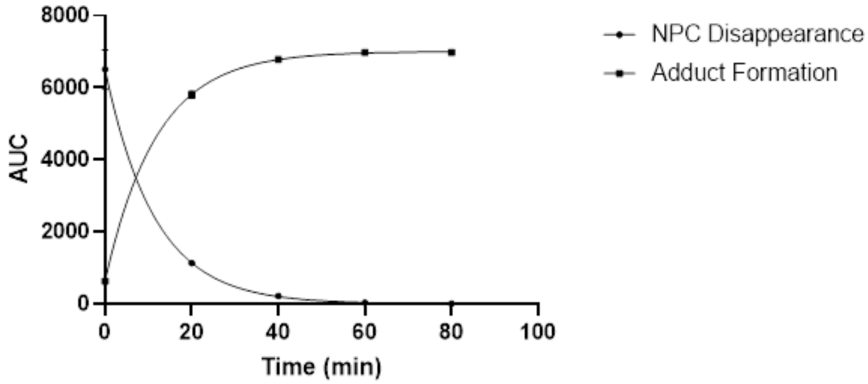

Figure S8. Plot of disappearance of NPC (1 mM) and formation of adduct for the addition of 1d (10 mM) vs time (min) in 67 mM CHES buffer (0.5% v/v DMSO) at pH 9.0, $\mu = 0.100$, T = 62°C. The area under the curve (AUC) was integrated from the chromatograph at 214 nm for the peaks corresponding to NPC and the adduct. The AUC data for disappearance of NPC were fitted to a mono-exponential decay with the constraint that the plateau = 0 and the data for formation of adduct were fitted to a mono-exponential association with the constraint that $Y_0 = 0$ to afford the k_{obs} values summarized in **Table S3**.

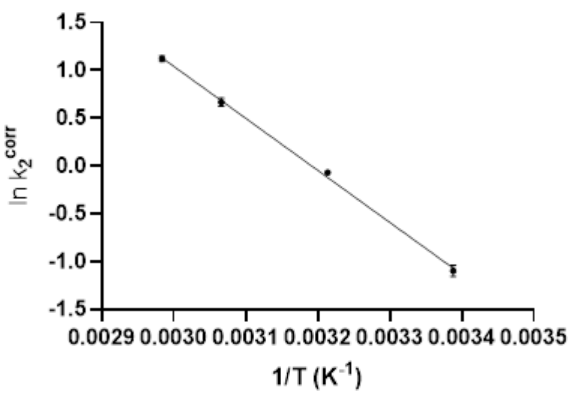

Figure S9. Arrhenius plot showing $\ln(k_2^{corr})$ vs 1/T for the addition of 1d to NPC in 67 mM CHES buffer (0.5% v/v DMSO), pH = 9.0, $\mu = 0.100$. The data were fitted to a linear regression to obtain a slope of -5440 ± 143 and y-intercept of 17.36 ± 0.45, $R^2 = 0.9986$.

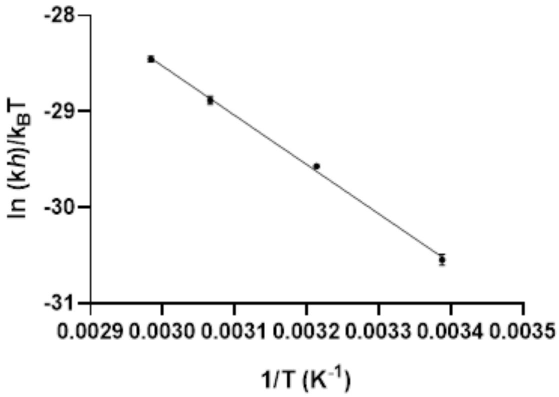

Figure S10. Eyring plot showing $\ln((k_2 h)/(k_B T))$ vs 1/T for the addition of 1d to NPC in 67 mM CHES buffer (0.5% v/v DMSO), pH = 9.0, μ = 0.100. The data were fitted to a linear regression to obtain a slope of -5126 ± 146 and y-intercept of -13.15 ± 0.46, $R^2 = 0.9984$.

Table S3. Observed rate constants (k_{obs}), calculated second order rate constants (k_2^{calc}), and corrected second order rate constants (k_2^{corr}) for the addition of MPA (**1d**) to NPC at variable temperatures. Measurements were made in duplicate for both the disappearance of acetamide and appearance of adduct. Errors represent the standard deviation of the replicate values.

Temp (°C)	k_{obs} (10^{-3} s^{-1})	k_2^{calc} ($M^{-1}s^{-1}$)	k_2^{corr} ($M^{-1}s^{-1}$)	$\ln(k_2^{corr})$	$\ln((k_2^{corr}h)/k_BT)$
22	0.1596 ± 0.0049	0.01596 ± 0.00049	0.3344 ± 0.0103	-1.0953 ± 0.0589	-30.543 ± 0.059
38	0.4460 ± 0.0116	0.04460 ± 0.00116	0.9345 ± 0.0243	-0.0678 ± 0.0255	-29.568 ± 0.026
52	0.9299 ± 0.0396	0.09299 ± 0.00396	1.9483 ± 0.0829	0.6670 ± 0.0432	-28.880 ± 0.043
63	1.4650 ± 0.0442	0.14650 ± 0.00442	3.0695 ± 0.0926	1.1215 ± 0.0304	-28.453 ± 0.030

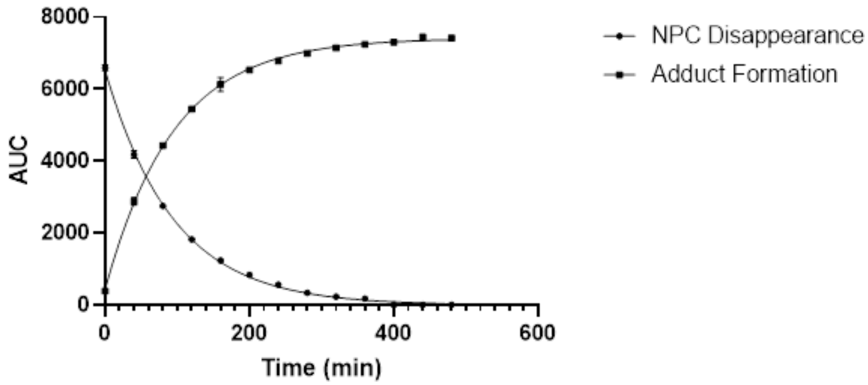

Figure S11. Plot of disappearance of NPC (1 mM) and formation of adduct for the addition of 1d (10 mM) vs time (min) in 67 mM CHES buffer (0.5% v/v DMSO), pH 9.0, $\mu = 0.050$, T = 22°C. The area under the curve (AUC) was integrated from the chromatograph at 214 nm for the peaks corresponding to NPC and the adduct. The AUC data for disappearance of NPC were fitted to a mono-exponential decay with the constraint that the plateau = 0 and the data for formation of adduct were fitted to a mono-exponential association with the constraint that $Y_0 = 0$ to afford the k_{obs} values summarized in **Table S4**.

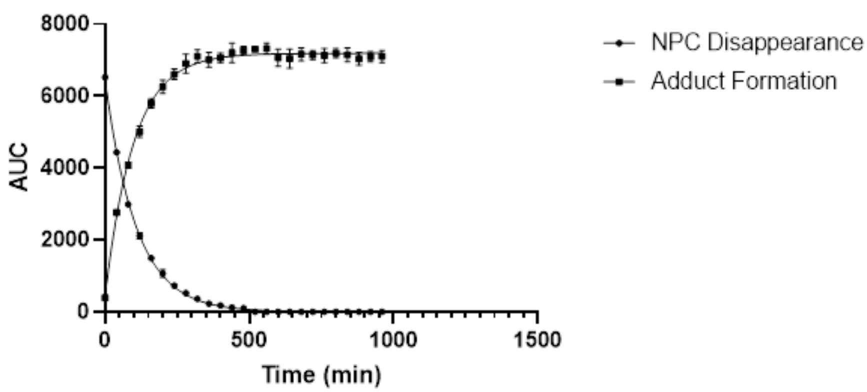

Figure S12. Plot of disappearance of NPC (1 mM) and formation of adduct for the addition of 1d (10 mM) vs time (min) in 67 mM CHES buffer (0.5% v/v DMSO), pH 9.0, $\mu = 0.075$, T = 22°C. The area under the curve (AUC) was integrated from the chromatograph at 214 nm for the peaks corresponding to NPC and the adduct. The AUC data for disappearance of NPC were fitted to a mono-exponential decay with the constraint that the plateau = 0 and the data for formation of adduct were fitted to a mono-exponential association with the constraint that $Y_0 = 0$ to afford the k_{obs} values summarized in **Table S4**.

Table S4. Observed rate constants (k_{obs}), calculated second order rate constants (k_2^{calc}), and corrected second order rate constants (k_2^{corr}) for the addition of MPA (**1d**) to NPC at varying ionic strengths. Measurements were made in duplicate for both the disappearance of acetamide and appearance of adduct. Errors represent the standard deviation of the replicate values.

[KCl] (M)	**k_{obs} (10^{-3} s^{-1})**	**k_2^{calc} ($M^{-1}s^{-1}$)**	**k_2^{corr} ($M^{-1}s^{-1}$)**
0.050	0.1834 ± 0.0070	0.01834 ± 0.00070	0.3843 ± 0.0146
0.075	0.1662 ± 0.0134	0.01662 ± 0.00134	0.3483 ± 0.0282
0.100	0.1596 ± 0.0049	0.01596 ± 0.00049	0.3344 ± 0.0103

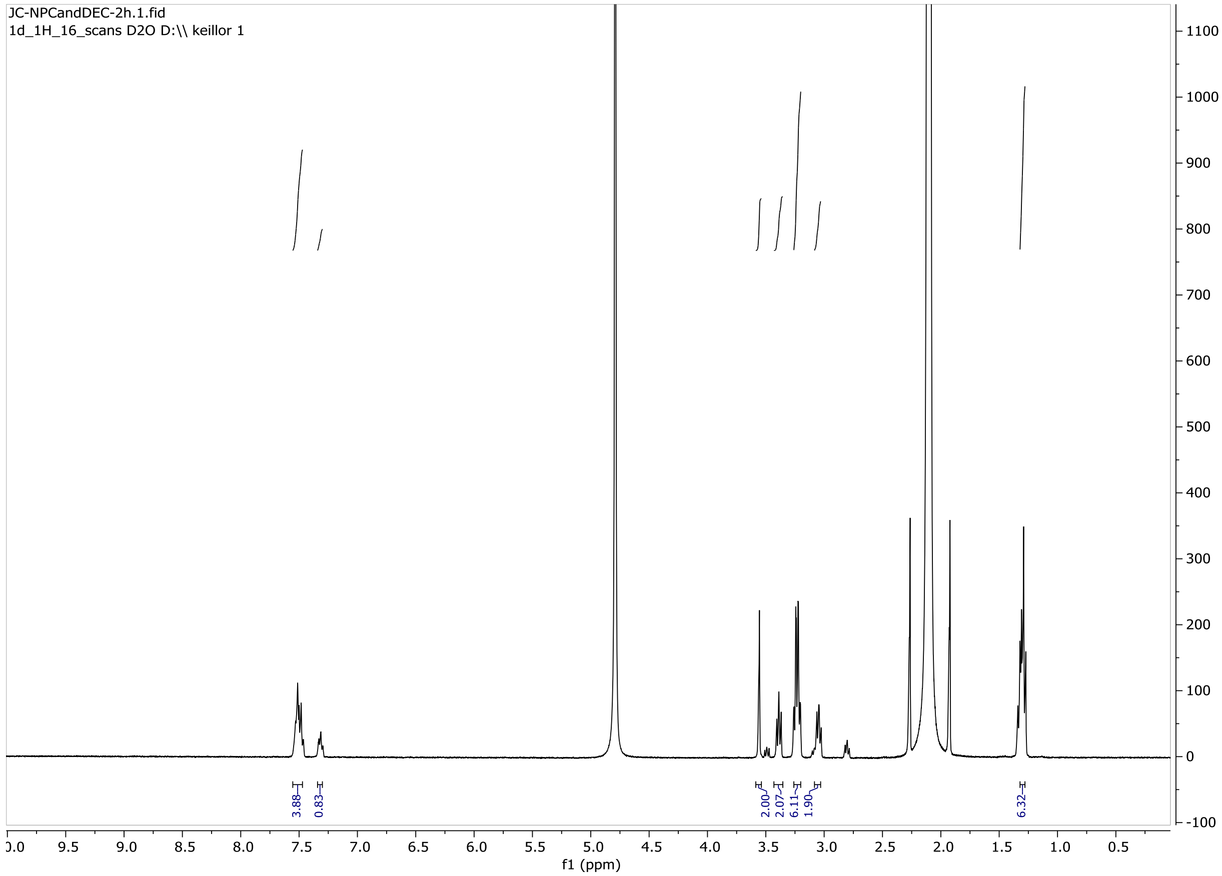

Figure S13. ^{1}H-NMR spectrum of adduct formed after 2 hours of allowing DEC to react with NPC in deuterated buffer.

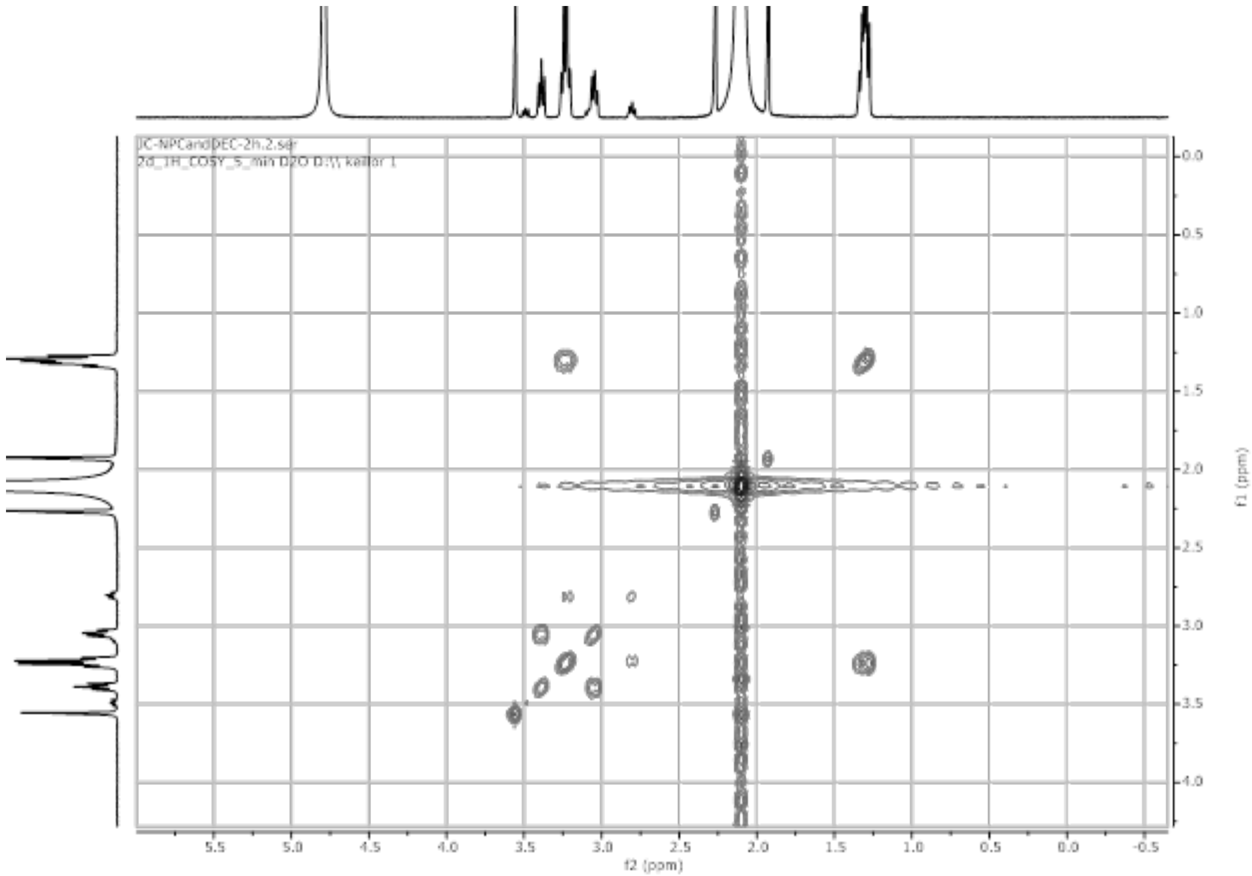

Figure S14: COSY spectrum of adduct formed after 2 hours of allowing DEC to react with NPC in deuterated buffer.

Table S5. Cartesian Coordinates of DFT-Calculated Structures

N-phenyl chloroacetamide

```
  19
  g98_logfile    structure: 23
  N      -0.455752   -0.102793   -0.000058
  C      -1.302676    0.943677    0.000067
  C      -2.794610    0.634774    0.000057
  H      -3.229492    1.090507   -0.885569
  O      -0.986920    2.120180    0.000190
  C       0.951625   -0.106150   -0.000046
  C       1.576787   -1.352996    0.000093
  C       1.725568    1.051331   -0.000163
  C       2.956647   -1.442926    0.000122
  H       0.976106   -2.254839    0.000187
  C       3.109871    0.944930   -0.000125
  H       1.249745    2.018163   -0.000274
  C       3.733695   -0.292169    0.000015
  H       3.425458   -2.418603    0.000231
  H       3.703943    1.850174   -0.000209
  H       4.813575   -0.361424    0.000045
  H      -0.890687   -1.013027   -0.000151
 Cl      -3.263235   -1.089767   -0.000074
  H      -3.229463    1.090364    0.885772
```

TS – methylthiolate chloroacetamide

```
24
  g98_logfile    structure: 32
  N       0.282585    0.412989   -0.480867
  C      -0.808840    0.278938    0.328099
  C      -2.100068    0.631393   -0.334896
  H      -2.997560    0.406353    0.209333
  O      -0.758291   -0.009131    1.512319
  C       1.626435    0.141188   -0.204261
  C       2.530882    0.261007   -1.263056
  C       2.100382   -0.231593    1.053567
  C       3.877508    0.014614   -1.069941
  H       2.171344    0.549563   -2.244025
  C       3.455272   -0.477048    1.231004
  H       1.412436   -0.327278    1.877251
  C       4.351751   -0.357623    0.181230
  H       4.559778    0.113563   -1.904834
  H       3.808912   -0.766425    2.212966
  H       5.405524   -0.551293    0.333088
  H       0.085519    0.642959   -1.440279
  H      -2.164635    0.762884   -1.398936
 Cl      -2.123882    2.735159    0.105895
  S      -2.221491   -1.866878   -0.922121
  C      -2.923518   -2.389323    0.670059
  H      -2.917376   -3.477385    0.750387
  H      -2.330809   -1.980800    1.491098
  H      -3.953878   -2.047004    0.784356
```

N-phenyl bromoacetamide

```
  19
  g98_logfile    structure: 23
  N       0.144468    0.104147   -0.000045
  C      -0.578164    1.240142   -0.000085
  C      -2.096144    1.119780   -0.000070
  H      -2.472993    1.622924   -0.885743
  O      -0.126044    2.371490   -0.000150
  C       1.542689   -0.058750    0.000013
  C       2.021885   -1.368829   -0.000130
  C       2.443204    1.003158    0.000134
  C       3.382631   -1.614834   -0.000117
  H       1.322919   -2.197189   -0.000239
  C       3.806428    0.740106    0.000159
  H       2.080393    2.017774    0.000186
  C       4.285452   -0.559870    0.000052
  H       3.737706   -2.637405   -0.000230
  H       4.499423    1.572051    0.000276
  H       5.350442   -0.751519    0.000068
  H      -0.387824   -0.752653   -0.000104
  H      -2.472956    1.623049    0.885552
 Br      -2.871655   -0.662954    0.000057
```

TS N-phenyl bromoacetamide

```
24
g98_logfile    structure: 35

N      -0.570415   -0.134609   -0.496951
C       0.466884    0.231542    0.310644
C       1.801165    0.194693   -0.361721
H       2.617562    0.636407    0.178267
O       0.360299    0.480809    1.499880
C      -1.938230   -0.188382   -0.209196
C      -2.796532   -0.516277   -1.262291
C      -2.476979    0.060505    1.053064
C      -4.161891   -0.593615   -1.059484
H      -2.385662   -0.710957   -2.246200
C      -3.850249   -0.020564    1.240419
H      -1.825086    0.314799    1.872337
C      -4.701030   -0.345820    0.196278
H      -4.807904   -0.848812   -1.890042
H      -4.254871    0.175592    2.225710
H      -5.769625   -0.405815    0.355999
H      -0.334038   -0.295873   -1.461497
H       1.881930    0.123044   -1.430790
Br      2.388932   -1.959386    0.048063
S       1.307157    2.706248   -0.906920
C       1.893857    3.338931    0.692707
H       1.605360    4.383495    0.820198
H       1.453036    2.760449    1.507301
H       2.980715    3.275913    0.774332
```

N-phenyl iodoacetamide

```
19
g98_logfile    structure: 24
N       0.855283   -0.086474    0.758031
C      -0.074335    0.897625    0.663244
C      -1.428330    0.525180    1.226817
H      -1.931435    1.420708    1.573218
O       0.120461    1.995472    0.175069
C       2.184709   -0.101136    0.299081
C       2.913474   -1.271323    0.516167
C       2.790431    0.973543   -0.347825
C       4.226359   -1.367042    0.093262
H       2.446370   -2.110246    1.018535
C       4.109362    0.861943   -0.766896
H       2.236369    1.881637   -0.518394
C       4.834587   -0.298834   -0.552570
H       4.775647   -2.282901    0.270189
H       4.570889    1.703006   -1.268960
H       5.862096   -0.372737   -0.883735
H       0.552205   -0.940466    1.197012
H      -1.387020   -0.219759    2.015439
I      -2.668176   -0.297310   -0.318826
```

TS N-phenyliodoacetamide

```
24
g98_logfile    structure: 64
N      -0.773390    0.006725   -0.423928
C       0.104121    0.489431    0.500640
C       1.340002    1.079621   -0.087842
H       1.958978    1.648908    0.579117
O      -0.063272    0.422551    1.706404
C      -2.038852   -0.558060   -0.219828
C      -2.875359   -0.666937   -1.332413
C      -2.483980   -1.025224    1.015792
C      -4.133315   -1.229057   -1.212898
H      -2.534701   -0.304289   -2.295321
C      -3.750408   -1.583151    1.121205
H      -1.845552   -0.946593    1.880245
C      -4.582194   -1.689826    0.017652
H      -4.766861   -1.303488   -2.087676
H      -4.085258   -1.941164    2.086888
H      -5.567513   -2.126983    0.112958
H      -0.549363    0.212121   -1.383378
H       1.423554    1.256657   -1.143697
I       2.813575   -0.927486   -0.105146
S      -0.001175    3.344799   -0.238674
C      -1.731993    3.002166    0.205213
H      -1.788174    2.353644    1.082264
H      -2.246526    3.934874    0.442378
H      -2.267501    2.515030   -0.611122
```

N-phenylacetamide thioether product

```
23
g98_logfile    structure: 31
N      -0.163819    0.064547   -0.327762
C      -0.965917    1.141443   -0.178166
C      -2.441596    0.908326   -0.495800
H      -2.608375    1.249495   -1.519544
O      -0.595384    2.255367    0.150540
C       1.224386   -0.050552   -0.150941
C       1.785575   -1.310445   -0.364050
C       2.045648    1.011935    0.219414
C       3.145661   -1.506115   -0.209084
H       1.148909   -2.138574   -0.653026
C       3.409308    0.799880    0.371683
H       1.619257    1.987580    0.385864
C       3.968415   -0.450222    0.160805
H       3.563760   -2.490190   -0.378500
H       4.039023    1.632226    0.660263
H       5.032802   -0.602647    0.282586
H      -0.648924   -0.783036   -0.592611
H      -3.018550    1.557162    0.161969
S      -3.069708   -0.777257   -0.419002
C      -3.015272   -1.057044    1.361831
H      -3.650475   -0.339308    1.878806
H      -3.394383   -2.062457    1.535855
H      -1.995153   -0.992135    1.738234
```

Table S6. Second order rate constants calculated according to Eyring transition state theory, using activation energies calculated for the reaction of *N*-phenylhaloacetamides with methanethiol

***N*-phenylhaloacetamide derivative**	**Calculated $k_2 = \frac{k_B T}{h} \exp\left(-\frac{\Delta G^{\ddagger}_{\text{calc}}}{k_B T}\right)$ ($M^{-1}s^{-1}$)**
Cl	6.07×10^{-5}
Br	1.07×10^{-1}
I	1.77×10^{-1}

Table S7. DFT-calculated activation energies for the reaction of *N*-phenylhaloacetamides with methanethiol in water and dichloromethane (DCM) solvents

***N*-phenylhaloacetamide derivative**	**Calculated $\Delta G^{\ddagger}$ (kcal/mol)**	
	Water	DCM
Cl	19.1	16.4
Br	14.7	12.3
I	14.4	5.9